levels is the more probable 5.58-MeV counterpart but does indicate the first substantial difference observed among the properties of the O^{18} and Ne^{24} nuclear structures.

In summary, it has been demonstrated that the low-lying levels of the Ne^{24} nuclear structure possess properties that are generally compatible with a simple two-body j-j-coupling shell-model representation involving essentially pure configurations. It thus appears that the effects of $1d_{5/2}$ subshell closure are important in the description of nuclei in this mass region, in which the existence of pronounced collective behavior has been previously well documented.

ACKNOWLEDGMENTS

The Yale authors wish to express their appreciation to Dr. D. E. Alburger for the hospitality extended to them at Brookhaven during the course of these measurements. Discussions with Dr. J. A. Becker concerning previous work on Ne^{24} are gratefully acknowledged. We also thank Dr. W. W. Watson for supplying the gas-target material used in these studies.

PHYSICAL REVIEW C VOLUME 1, NUMBER 4 APRIL 1970

Study of the (d, t) Reaction on Si^{28}, S^{32}, and Ar^{36}†

C. A. WHITTEN, JR.,* M. C. MERMAZ,‡ AND D. A. BROMLEY
Wright Nuclear Structure Laboratory, Yale University, New Haven, Connecticut 06520

(Received 19 November 1969)

The $Si^{28}(d, t)Si^{27}$ reaction and the $S^{32}(d, t)S^{31}$ and $Ar^{36}(d, t)Ar^{35}$ reactions were studied at deuteron energies of 21.6 and 21.0 MeV, respectively. Angular distributions were obtained for triton groups from these (d, t) reactions leading to levels in the residual nuclei Si^{27}, S^{31}, and Ar^{35} with excitation energies up to approximately 3.5 MeV. Spectroscopic factors for the strong (d, t) transitions were extracted using now standard distorted-wave Born-approximation (DWBA) analyses. The (d, t) spectroscopic factors from this work are in reasonable agreement with previous neutron-pickup experimental data on Si^{28}, S^{32}, and Ar^{36}, whenever the latter are available. Recent $2s$-$1d$ shell-model calculations are in reasonable accord with these data. In the particular case of the $Ar^{36}(d, t)Ar^{35}$ data, it appears that the theoretical calculation which uses a "realistic" interaction derived from nucleon-nucleon scattering gives better agreement with these data than the theoretical calculation which uses a modified surface δ interaction.

I. INTRODUCTION

THIS paper represents the second in a series of three papers dealing with deuteron induced reactions on the even-even, $T=0$, target nuclei Si^{28}, S^{32}, and Ar^{36}, which lie in the upper half of the s-d shell. The first paper[1] in this series presented data for the (d, d) and (d, d') reactions on the above mentioned nuclei, while the present work and the third paper[2] present data for the (d, t) and (d, p) reactions, respectively. The general purpose of this series of experiments has been to investigate the equilibrium shape of these nuclei using the (d, d') reaction and also to investigate the neutron hole and neutron particle structure relative to these even-even cores with the (d, t) and (d, p) reactions, respectively. In the case of Si^{28} it had been suggested[3] that the combination of single nucleon pickup and stripping reactions on this target nucleus could be used to study possible changes in the equilibrium shape of the core as a nucleon is either added to or subtracted from that core.

Considerable data have been reported for the single neutron pickup reactions (p, d) [4–6] and (He^3, α) [7–9] on Si^{28}, S^{32}, and Ar^{36}; the present work, however, represents the first study of the (d, t) reaction on these target nuclei. The very large neutron binding energies for these even-even, $T=0$, target nuclei—ranging from 15.09 MeV in S^{32} to 17.18 MeV in Si^{28}—made it necessary to use incident deuteron energies of $\sim$21 MeV in order to study a reasonable range of excitation

† Work supported in part by the U.S. Atomic Energy Commission under Contract No. AT(30-1)3223.

* Present address: Department of Physics, University of California, Los Angeles, Calif. 90024.

‡ NATO Fellow on leave of absence from the Center of Nuclear Research, Saclay, France. Present address: Center of Nuclear Research, Saclay, France.

[1] M. C. Mermaz, C. A. Whitten, Jr., and D. A. Bromley, Phys. Rev. **187**, 1466 (1969).

[2] M. C. Mermaz, C. A. Whitten, Jr., J. W. Champlin, A. J. Howard, and D. A. Bromley (to be published).

[3] G. Ripka, in *Proceedings of the International Nuclear Physics Conference, Gatlinburg, Tennessee, 1966* (Academic Press, Inc., New York, 1967), p. 833.

[4] G. D. Jones, R. R. Johnson, and R. J. Griffiths, Nucl. Phys. **A107**, 659 (1968).

[5] R. R. Johnson and R. J. Griffiths, Nucl. Phys. **A108**, 113 (1968).

[6] R. L. Kozub, Phys. Rev. **172**, 1078 (1968).

[7] B. H. Wildenthal and P. W. M. Glaudemans, Nucl. Phys. **A92**, 353 (1967).

[8] L. W. Swenson, R. W. Zurmühle, and C. M. Fou, Nucl. Phys. **A90**, 232 (1967).

[9] C. M. Fou and R. W. Zurmühle, Phys. Rev. **151**, 927 (1966).

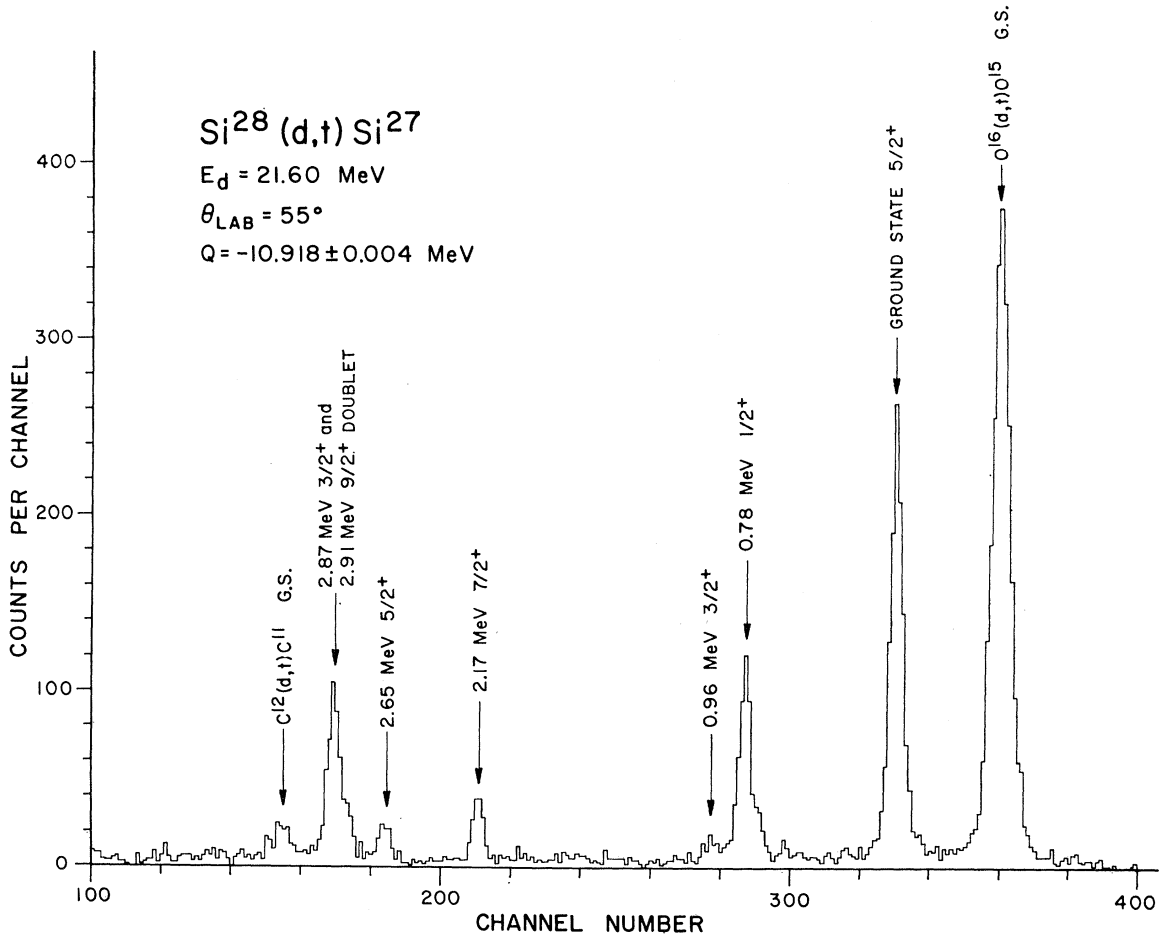

FIG. 1. Triton spectrum from the $Si^{28}(d, t)Si^{27}$ reaction with $E_d = 21.6$ MeV and $\theta_{lab} = 55°$.

energy in the residual nucleus. The recently reported (p, d) reaction studies on Si^{28}, S^{32}, and Ar^{36} were performed at incident proton energies between 27.5 and 33.6 MeV, while the (He^3, α) reaction studies were performed at incident helium-3 energies between 10 and 15 MeV.

The experimental (d, t) angular distributions measured in this experiment are presented in Sec. III, while the distorted-wave Born-approximation (DWBA) analyses used to fit these experimental data are discussed in Sec. IV. The spectroscopic information resulting from these DWBA analyses is presented in Sec. V; and comparisons are made with the results of the previously mentioned (p, d) and (He^3, α) reaction studies. Recently an extensive series of shell model calculations in the *s-d* shell region has been performed by Halbert, Glaudemans, McGrory, and Wildenthal at the Oak Ridge National Laboratory.[10] Within an *s-d* shell basis the energy level structure for nuclei with $17 \leq A \leq 39$ is determined, as well as the spectroscopic factors for single nucleon transfer reactions such as (d, t) and (d, p). These theoretical calculations are compared with the present (d, t) experimental results in Sec. V.

In the deuteron elastic and inelastic scattering studies[1] previously reported we have adduced evidence for a stable oblate equilibrium deformation for Si^{28} and spherical equilibrium configurations for S^{32} and Ar^{36}. The present complementary studies, while consistent with this interpretation, do not provide strong supportive evidence.

II. EXPERIMENTAL PROCEDURE

The (d, t) experiments reported herein were performed in a 30-in. Ortec scattering chamber using 21.60- and 21.00-MeV deuteron beams from the Yale MP tandem Van de Graaff accelerator. Typical deuteron beam intensities varied between 20 nA for measurements at the most forward angle (15°) to 750 nA for measurements at angles past 60°. A ΔE-E telescope of silicon surface-barrier detectors (140 μ for ΔE, 530 μ for E), standard electronics, and a Landis-Goulding

[10] E. Halbert, in *Proceedings of the Third International Symposium on the Structure of Low Medium Mass Nuclei* (University of Kansas, Lawrence, Kansas, 1968).

particle identifier,[11] the latter fabricated in this laboratory, identified and energy analyzed the triton groups of interest. The triton spectra were stored in a standard 1024-channel analyzer.

In the $Si^{28}(d, t)$ experiment performed at 21.60 MeV a self-supported foil of natural silicon (Si^{28} 92.7% abundant) oxide was used. This foil was a mixture of the chemical forms SiO and SiO_2 and was approximately 400 $\mu g/cm^2$ thick. In the $S^{32}(d, t)$ and $Ar^{36}(d, t)$ experiments performed at 21.00 MeV, a gas cell target was used. The wall of the gas cell was 0.1-mil Havar foil[12]; a two collimator system, consisting of a vertical front slit and a circular back aperture, defined the effective interaction volume in the gas cell. The sulfur target was H_2S gas (S^{32} 95.0% abundant) purchased from a commercial source, while the A^{36} gas was separated by the Yale Isotope Separation Group and was made available for these experiments by Dr. A. Howard and Dr. W. W. Watson, to whom we are much indebted. The gas cell pressures were typically 20–30 cm Hg. During all runs the target condition was monitored by an additional surface barrier counter which detected elastic deuteron scattering events.

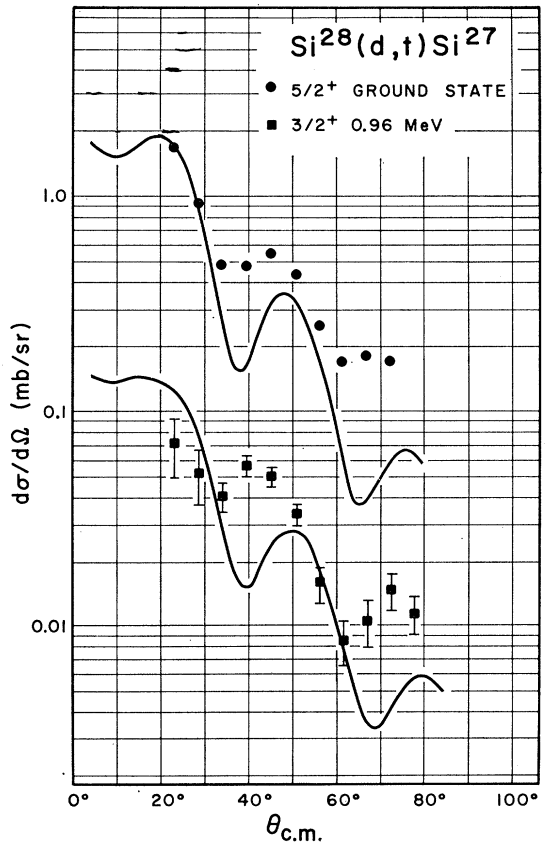

FIG. 2. Experimental $Si^{28}(d, t)Si^{27}$ angular distributions for the $\frac{5}{2}^+$ ground state and the $\frac{3}{2}^+$ 0.96-MeV level. The solid curves represent $l_n=2$ ($1d$) DWBA fits to the experimental data.

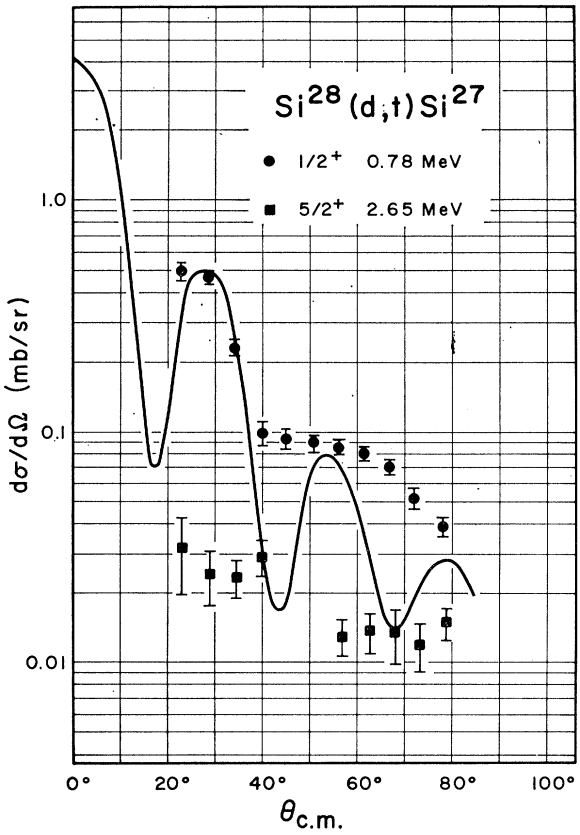

FIG. 3. Experimental $Si^{28}(d,t)Si^{27}$ angular distributions for the $\frac{1}{2}^+$ 0.78-MeV level and the $\frac{5}{2}^+$ 2.65-MeV level. The solid curve represents an $l_n=0$ ($2s_{1/2}$) DWBA fit to the experimental data for the $\frac{1}{2}^+$ 0.78-MeV level.

In the $Si^{28}(d, t)$ experiment the absolute cross sections were determined by measuring the (d, t) yields at $E_d=21.60$ MeV under the same experimental conditions as used to measure the elastic deuteron scattering yield from the same silicon target at $E_d=18.00$ MeV. The absolute deuteron elastic cross sections on silicon at this energy had been measured in a previous experiment.[1] A conservative estimate of the accuracy of the $Si^{28}(d, t)$ absolute cross sections determined by this method is $\pm 20\%$, excluding counting statistics. However, since the silicon target condition and beam intensity were continuously monitored using the monitor detector system the accuracy of the relative $Si^{28}(d, t)$ differential cross sections is significantly better, being mainly limited by the counting statistics. During the series of runs the ratio of elastically scattered deuteron monitor counts to integrated beam charge remained constant; no evidence for any deterioration of the silicon target was detected.

In the $S^{32}(d, t)$ and $Ar^{36}(d, t)$ experiments the primary difficulty in determining accurate absolute cross sections was the uncertainty in the gas density along

[11] F. S. Goulding, D. A. Landis, J. Cerny, and R. J. Pehl, Nucl. Instr. Methods **31**, 1 (1964).
[12] Hamilton Watch Co., Lancaster, Pa.

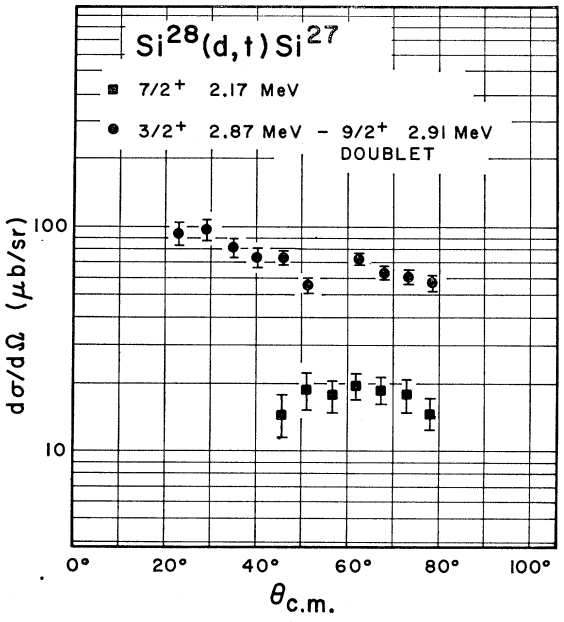

FIG. 4. Experimental $Si^{28}(d, t)Si^{27}$ angular distributions for the $\frac{7}{2}^+$ 2.17-MeV level and the unresolved $\frac{3}{2}^+$ 2.87-MeV–$\frac{9}{2}^+$ 2.91-MeV doublet.

the beam path reflecting local gas heating by the beam. In the $Ar^{36}(d, t)$ experiment we were able to estimate this effect quite accurately by plotting the deuteron elastic monitor counts per microcoulomb of beam as a function of the beam intensity and extrapolating this curve to zero beam current (or no heating effect). In the $S^{32}(d, t)$ experiment the H_2S gas was cracked by the beam—mainly at the entrance and exit foils of the gas cell—so that the gas density in the cell decreased monotonically as a function of time. This cracking effect was monitored by analyzing the H_2S gas sample before and after a series of runs. After a series of runs representing approximately 2500 μC of integrated charge at beam currents between 10 and 300 nA, the amount of hydrogen gas in the sample had increased by a factor of 30. The monotonic decrease in the gas density due to this cracking effect made it difficult to determine the local heating effect with good accuracy. Conservative estimates of the accuracy of the $S^{32}(d, t)$ and $Ar^{36}(d, t)$ absolute cross sections are ± 15 and $\pm 8\%$, respectively, excluding counting statistics. However, as in the $Si^{28}(d, t)$ experiment, the use of a monitor detector to continuously monitor the target condition allows the relative (d, t) cross sections in these two gas cell experiments to be determined to a much higher degree of accuracy (mainly statistically limited).

III. EXPERIMENTAL RESULTS

A. $Si^{28}(d, t)Si^{27}$

At an incident deuteron energy of 21.60 MeV, $Si^{28}(d, t)$ data were obtained for laboratory angles between 20° and 70°. Figure 1 presents the triton spectrum obtained at a laboratory angle of 55°. The experimental energy resolution was approximately 70 keV. All known levels in Si^{27} up to an excitation energy of 3 MeV were excited with some strength in this experiment. The Si^{27} excitation energies shown in Fig. 1 were taken from a $Si^{28}(He^3, \alpha)Si^{27}$ experiment[13] which used a magnetic spectrograph. In most cases, the spin assignments were taken from the compilation of Endt and Van der Leun[14]; in some cases spin assignments were made by comparing the level diagram of Si^{27} $(T_z=-\frac{1}{2})$ with that of its $T_z=+\frac{1}{2}$ mirror nucleus Al^{27}.[14] The use of a silicon oxide target resulted in a very strong triton group from $O^{16}(d, t)O^{15}$ ground-state reaction which obscured the $Si^{28}(d, t)Si^{27}$ ground-state triton group at $\theta_{lab}=70°$. A small carbon contamination in the target produced a rather weak $C^{12}(d, t)C^{11}$ ground-state triton group which, as it moved kinematically across the spectrum, interfered in turn at one or two angles with each of the Si^{27} triton groups with excitation energies between 2 and 3 MeV.

Figures 2–4 present the $Si^{28}(d, t)Si^{27}$ angular distributions measured in this experiment. The error bars on these data and on all succeeding experimental data represent only statistical errors and errors in the background subtraction; they do not include the error in the normalization of the absolute cross section discussed in Sec. II. Except possibly at the most forward angle ($\theta_{lab}=20°$), the angular distributions to the $\frac{5}{2}^+$ ground state and the $\frac{3}{2}^+$ 0.96-MeV level (Fig. 2) are quite similar and indicate $l_n=2$ pickup transitions. The transition to the $\frac{3}{2}^+$ 0.96-MeV level is quite weak and the experimental statistics, particularly at the forward angles, are poor. The angular distribution to the $\frac{1}{2}^+$ 0.78-MeV level (Fig. 3) has an $l_n=0$ pickup shape. Data for the $\frac{7}{2}^+$ 2.17-MeV level could be obtained only for angles greater than 35° because of the experimental background and the interference from the $C^{12}(d, t)C^{11}$ ground-state group. For laboratory angles between 40° and 70° the angular distribution to this level is quite isotopic (Fig. 4). Since this $\frac{7}{2}^+$ level would not be excited by a first-order direct reaction mechanism, its $\sim$20-μb/sr cross section between 40° and 70° gives some indication of the cross sections due to second order direct and/or compound nuclear reaction mechanisms in this mass and energy region. The angular distribution to the $\frac{5}{2}^+$ 2.65-MeV level (Fig. 3) shows some forward peaking, but the weakness of this transition makes the assignment of an $l_n=2$ pickup shape very tenuous. The data points at $\theta_{lab}=40°$ and 45° for the $\frac{5}{2}^+$ 2.65-MeV level were blocked by the $C^{12}(d, t)C^{11}$ ground-state group. The angular distribution to the $\frac{3}{2}^+$ 2.87-MeV and $\frac{9}{2}^+$ 2.91-MeV doublet, which was unresolved in this experiment, is quite interesting

[13] S. Hinds and R. Middleton, Proc. Phys. Soc. (London) **73**, 727 (1959).
[14] P. M. Endt and C. Van der Leun, Nucl. Phys. **A105**, 1 (1968).

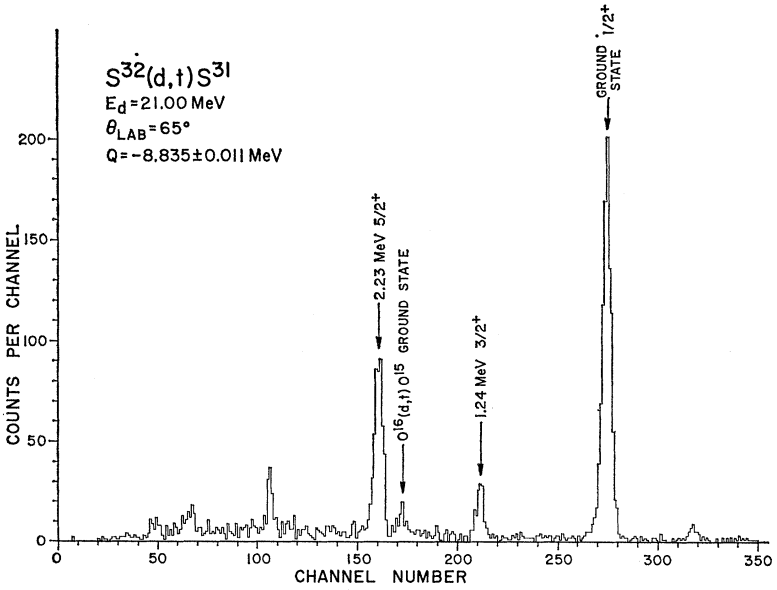

FIG. 5. Triton spectrum from the $S^{32}(d, t)S^{31}$ reaction with $E_d=21.00$ MeV and $\theta_{lab}=65°$.

(Fig. 4). The cross section to this doublet is large, but the angular distribution falls off very slowly with increasing angle and does not resemble an $l_n=2$ pickup shape. This most probably indicates that both the $\frac{3}{2}^+$ 2.87-MeV level, whose angular distribution could have an $l_n=2$ pickup shape, and the $\frac{9}{2}^+$ 2.91-MeV level, which would be excited by second-order direct and/or compound nuclear reaction mechanisms, are being excited with some strength in this (d, t) experiment. In a $Si^{28}(d, He^3)Al^{27}$ experiment performed at $E_d=16.1$, 17.0, 18.0, and 20.0 MeV [15] it was found that the $\frac{9}{2}^+$ 3.000-MeV level in Al^{27} was excited more strongly than the $\frac{3}{2}^+$ 2.976-MeV level. The general characteristics of the $Si^{28}(d, t)Si^{27}$ angular distributions presented here agree with the previous (p, d) [4,6] and (He^3, α) [7,8,16] neutron pickup studies on Si^{28}; however, most of these studies found a more definite $l_n=2$ pickup shape for the angular distribution to the $\frac{5}{2}^+$ 2.65-MeV level and found that the angular distribution to the $\frac{3}{2}^+$ 2.87-MeV and $\frac{9}{2}^+$ 2.91-MeV doublet has a definite $l_n=2$ pickup shape.

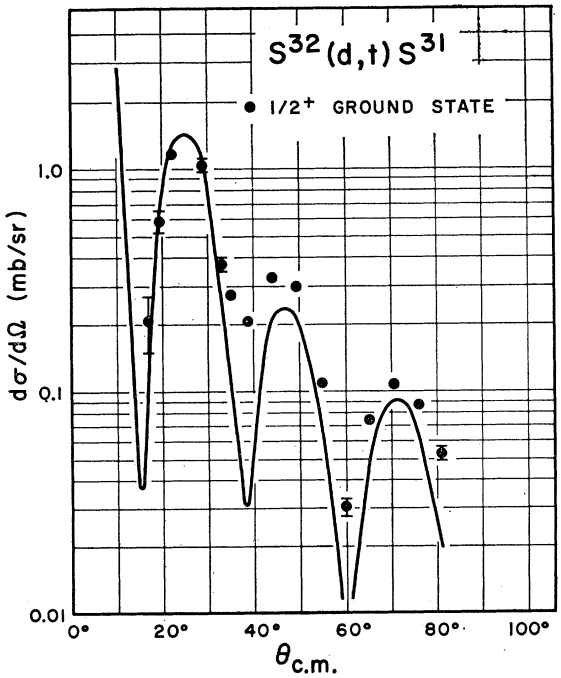

FIG. 6. Experimental $S^{32}(d, t)S^{31}$ angular distribution for the $\frac{1}{2}^+$ ground state. The solid curve represents an $l_n=0$ $(2s_{1/2})$ DWBA fit to the experimental data.

B. $S^{32}(d, t)S^{31}$

At an incident deuteron energy of 21.00 MeV, $S^{32}(d, t)S^{31}$ data were obtained between laboratory angles of 15° and 75°. Figure 5 presents the triton spectrum obtained at a laboratory angle of 65°. The experimental energy resolution was typically 90–100 keV. The (d, t) transitions to the ground state and first two excited states of S^{31} were studied in the present work. The excitation energies and spin and parity assignments for these three levels were taken from the *s-d* shell compilation of Endt and Van der Leun.[14] A small air contamination in the H_2S gas target produced a weak $O^{16}(d, t)O^{15}$ ground-state triton group which interfered with the data for the $\frac{3}{2}^+$ 1.24-MeV level at $\theta_{lab}=40°$. Figures 6 and 7 present the $S^{32}(d, t)S^{31}$ angular distributions measured in this experiment. The angular distribution to the $\frac{1}{2}^+$ ground state of S^{31} (Fig. 6) has an $l_n=0$ pickup shape, while the angular dis-

[15] H. E. Gove, K. H. Purser, J. J. Schwartz, W. P. Alford, and D. Cline, Nucl. Phys. **A116**, 369 (1968).

[16] S. Hinds and R. Middleton, Proc. Phys. Soc. (London) **75**, 444 (1960).

TABLE I. Optical model parameters used in the DWBA analysis of the experimental (d, t) angular distributions.

$$V(r) = U(r) - V_0(1+e^x)^{-1} - iW_0(1+e^{x'})^{-1} + 4W'(d/dx')(1+e^{x'})^{-1}$$

where

$$U_c(r) = (Ze^2/2r_{0c}A^{1/3})[3-(r/r_{0c}A^{1/3})^2]; \quad r<r_{0c}A^{1/3}$$
$$U_c(r) = Ze^2/r; \quad r>r_{0c}A^{1/3}$$
$$x=(r-r_{0c}A^{1/3})/a; \quad x'=(r-r'_0A^{1/3})/a'$$

	V_0	r_0	r_{0c}	a	W_0	W' [b]	r'_0	a'
1. Deuteron parameters[a]								
d+Si^{28}	123.0	0.89	1.30	0.945	...	109.2	1.385	0.539
d+S^{32}	110.87	1.005	1.30	0.8737	...	82.04	1.417	0.585
d+A^{36}	86.41	1.215	1.30	0.513	...	43.6	1.66	0.592
2. Triton parameters[c]	147.1	1.40	1.30	0.61	54.1	...	1.40	0.61
3. Neutron well parameters	$r_{0n}=1.25$ F, $a=0.65$, $\lambda=25.00$							

[a] Reference 1.
[b] $W'=4W_D$. W_D is the parameter often quoted in the literature. W' is the value we put in the DWBA computer program JULIE.
[c] Reference 23.

tributions to the $\frac{3}{2}^+$ 1.24-MeV and $\frac{5}{2}^+$ 2.23-MeV levels (Fig. 7) have $l_n=2$ pickup shapes. These l_n assignments are in agreement with previous (p, d) [6,17] and (He^3, α) [9,18] neutron pickup studies on S^{32}.

C. Ar$^{36}(d, t)$Ar^{35}

At an incident deuteron energy of 21.00 MeV, Ar$^{36}(d, t)$Ar^{35} data were obtained between laboratory angles of 15° and 80°. Figure 8 presents the triton spectrum obtained at a laboratory angle of 30°. The experimental energy resolution was typically 65–70 keV. An arrow in Fig. 8 marks the ΔE line in the triton spectrum—tritons with energies less than this amount stop in the 140-μ ΔE detector. In this experiment angular distributions could have been obtained for levels in Ar^{35} up to an excitation energy of approximately 5 MeV. However, no levels in Ar^{35} above an excitation energy of 3.2 MeV were populated with appreciable yield. Since the excitation energies for levels in Ar^{35} were not known accurately,[14] an energy calibration curve was established in this experiment to determine the excitation energies to good accuracy. Under the same experimental conditions as in the Ar$^{36}(d, t)$ runs, data on the Ne$^{22}(d, t)$Ne^{21} reaction were taken at a number of angles. The peak positions of the Ne^{21} ground state, the 0.350-MeV and the 1.747-MeV levels were then used to construct a triton energy calibration curve. At forward angles in the Ar$^{36}(d, t)$ runs, the O$^{16}(d, t)$O^{15} ground-state triton group was detected, reflecting a very small oxygen contaimination in the Ar^{36} gas, and its peak positions were used to establish additional points on the triton energy calibration curve. Using this calibration curve the Q value for the Ar$^{36}(d, t)$Ar^{35} reaction was determined to be -9.007 ± 0.010 MeV, in good agreement with the published value of -8.895 ± 0.017 MeV. The excitation energies of the Ar^{35} levels studied in this experiment were determined to be 1.180 ± 0.010 MeV, 2.635 ± 0.020 MeV, 2.985 ± 0.020 MeV, and 3.200 ± 0.020 MeV. These excitation energies are in good agreement with those obtained from other Ar^{35} studies.[5,6] A level in Ar^{35} has been reported at 1.70 ± 0.03 MeV.[6] The spin of this level should be $\frac{5}{2}^+$, as its analog in Cl^{35} at 1.762 MeV

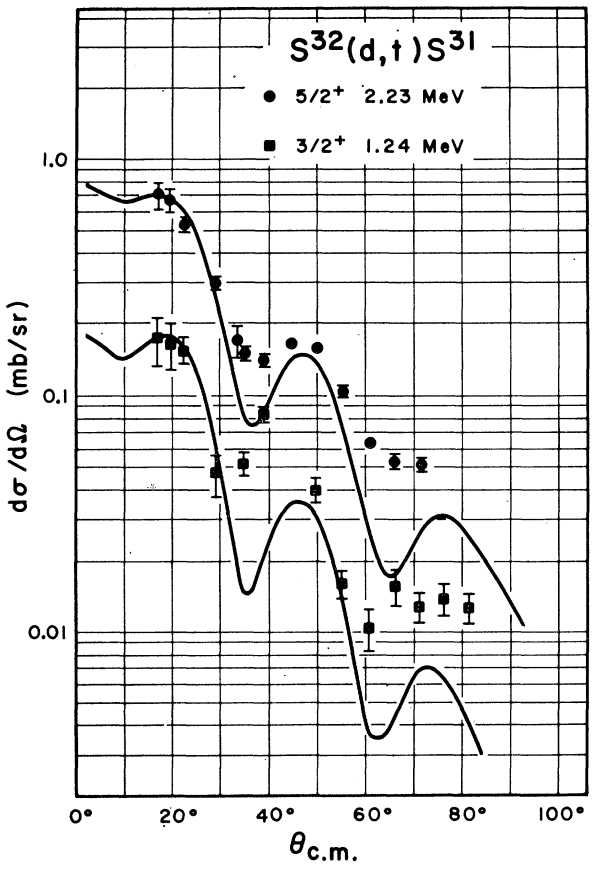

FIG. 7. Experimental S$^{32}(d, t)$S^{31} angular distributions for the $\frac{3}{2}^+$ 1.24-MeV level and the $\frac{5}{2}^+$ 2.23-MeV level. The solid curves represent $l_n=2$ $(1d)$ DWBA fits to the experimental data.

[17] C. Glashausser and M. Rickey, Phys. Rev. **154**, 1033 (1967).
[18] C. E. Moss, thesis, California Institute of Technology, 1968 (unpublished).

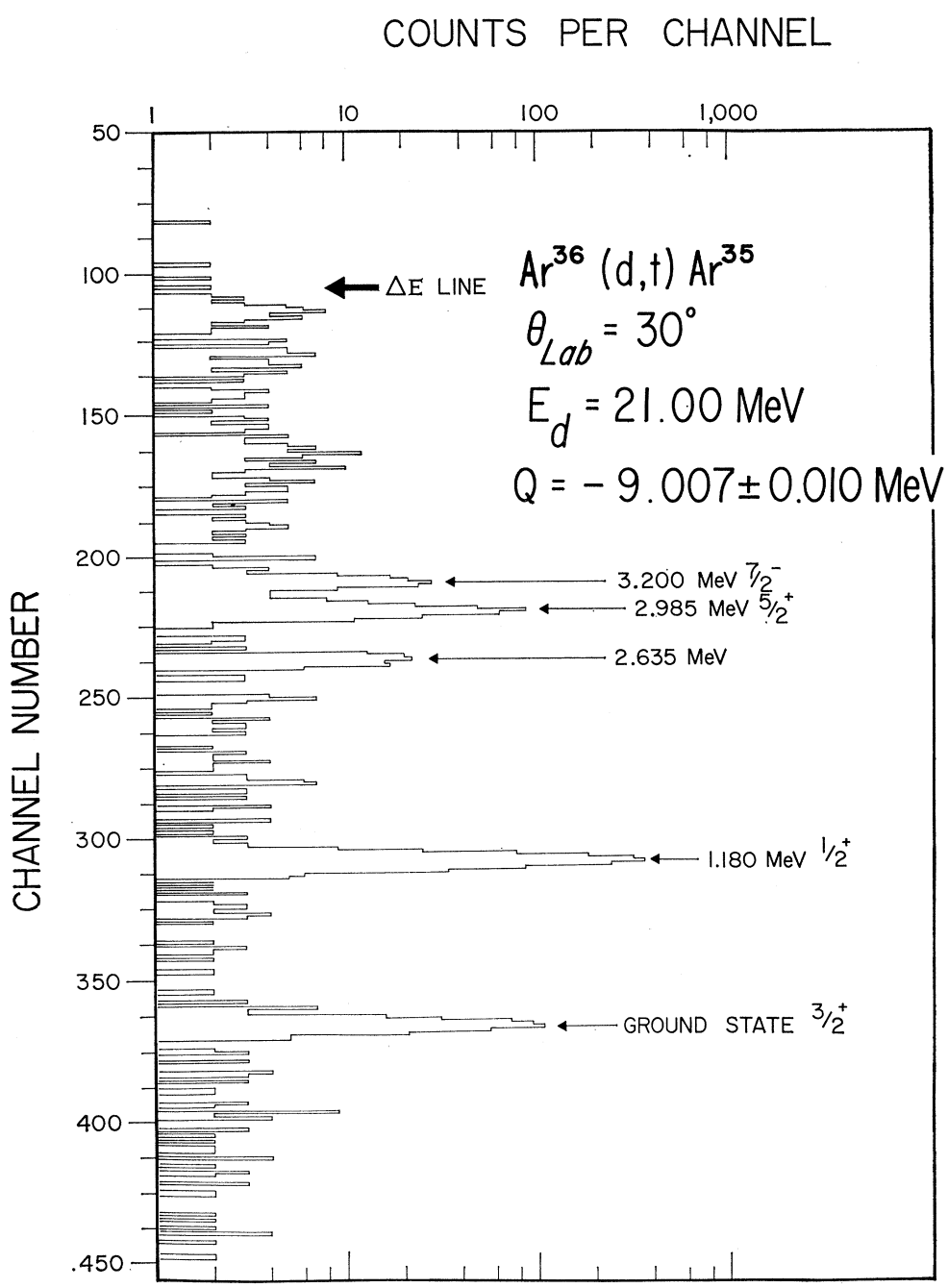

FIG. 8. Triton spectrum from the $Ar^{36}(d, t)A^{35}$ reaction with $E_d=21.00$ MeV and $\theta_{lab}=30°$.

is known to be a $\frac{5}{2}^+$ level.[14] This state is excited extremely weakly in the present $Ar^{36}(d, t)Ar^{35}$ work. The (d, t) cross section to this level is less than 7 μb/sr for laboratory angles between 30° and 80°.

Figures 9–11 present the $Ar^{36}(d, t)Ar^{35}$ angular distributions measured in this experiment. The angular distributions to the $\frac{3}{2}^+$ ground state and the 2.985-MeV level of Ar^{35} (Fig. 9) show characteristic $l_n=2$ pickup shapes. The spin of the 2.985-MeV level is very probably $\frac{5}{2}^+$, since its analog in Cl^{35} at 3.006 MeV has been tentatively assigned spin $\frac{5}{2}$ [19] and its excitation energy fits well with the systematic position of the main $1d_{5/2}$ neutron hole strength as observed in Si^{27} and S^{31}. The angular distribution to the $\frac{1}{2}^+$ 1.180-MeV level (Fig. 10) shows a characteristic $l_n=0$ shape. Considerable structure and forward peaking is exhibited by the (d, t)

[19] P. Taras, L. W. Oleksiuk, R. E. Azuma, and J. D. Prentice, Phys. Rev. **164**, 1386 (1967).

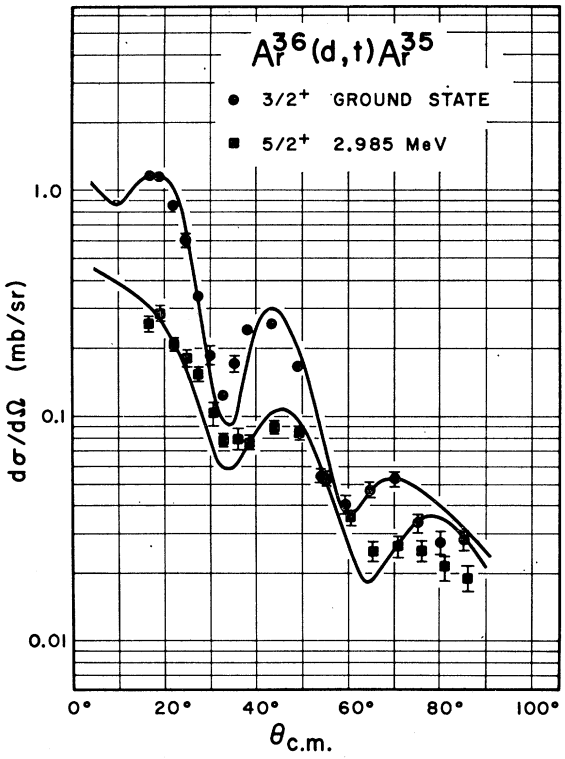

FIG. 9. Experimental $Ar^{36}(d, t)Ar^{35}$ angular distributions for the $\frac{3}{2}^+$ ground state and the $\frac{5}{2}^+$ 2.985-MeV level. The solid curves represent $l_n=2$ ($1d$) DWBA fits to the experimental data.

angular distribution to the 2.635 MeV level of Ar^{35} (Fig. 11). A doublet would be expected in Ar^{35} at about this excitation energy, since its mirror nucleus Cl^{35} has levels at 2.645 and 2.695 MeV.[14] However, when the energy calibration curve discussed previously is used to predict the Q value corresponding to this $Ar^{36}(d, t)Ar^{35}$ triton group, the predicted Q value varies by less than 4 keV between $\theta_{lab}=30°$ and 70°. This implies that this experimental triton group either corresponds to a very close lying doublet in Ar^{35} or that only one member of a possible doublet is being excited with any appreciable strength in the $Ar^{36}(d, t)Ar^{35}$ reaction. As is discussed in Sec. IV, we have attempted to fit the angular distribution to the 2.635-MeV level with DWBA curves assuming either $l_n=2$ ($1d_{3/2}$) or $l_n=1$ ($2p_{3/2}$) neutron pickup.

The angular distribution to the 3.200-MeV level in Ar^{35} (Fig. 11) shows some forward peaking. The spin-parity assignment for this level is almost certainly $\frac{7}{2}^-$, since its analog in Cl^{35} at 3.163 MeV has been given a definite assignment of $\frac{7}{2}^-$.[19,20] As will be discussed in Sec. IV, we have attempted to fit this angular distribution with a DWBA curve which assumes $l_n=3$ ($1f_{7/2}$) neutron pickup.

[20] D. D. Watson, Phys. Letters **22**, 183 (1966).

IV. DWBA ANALYSES

Distorted-wave Born-approximation (DWBA) analyses were performed using the Oak Ridge computer code JULIE[21,22] in order to obtain spectroscopic information from the experimental (d, t) angular distributions. The deuteron and triton optical model parameters used in these analyses, as well as the bound neutron well parameters, are presented in Table I. The deuteron optical model parameters were those obtained from a study of 18-MeV deuteron elastic scattering on Si^{28}, S^{32}, and Ar^{36}.[1] The triton optical model parameters were those obtained by Glover and Jones from an analysis of 12-MeV triton elastic scattering on Al^{27}.[23] No spin-orbit terms were included in either the deuteron or triton optical model potentials.

In most of the DWBA calculations the bound neutron wave function, or form factor, was calculated using a Woods-Saxon potential where the radius parameter r_{0n}, the diffuseness parameter a, and the spin-orbit

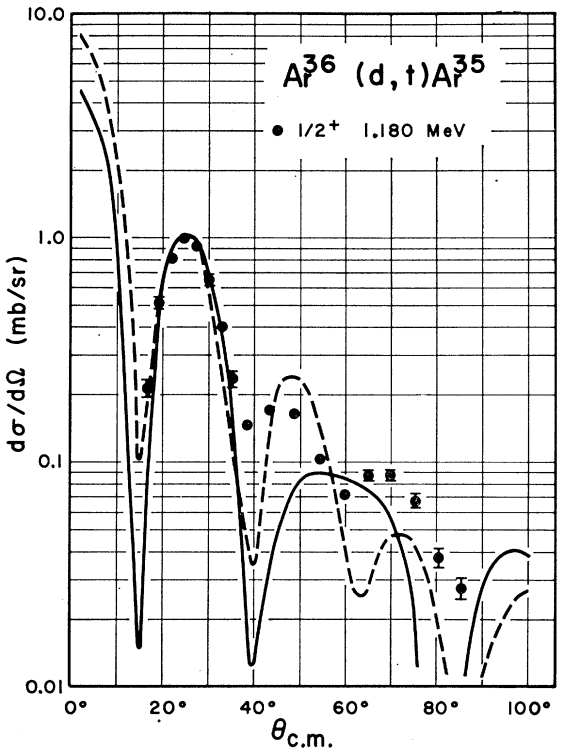

FIG. 10. Experimental $Ar^{36}(d, t)Ar^{35}$ angular distribution for the $\frac{1}{2}^+$ 1.18-MeV level. The experimental data are fitted with two $l_n=0$ ($2s_{1/2}$) curves. In the solid curve the d+Ar^{36} optical model parameters of Table I are used, while in the dotted curve deuteron optical model parameters similar to the d+Si^{28} parameters of Table I are used.

[21] R. H. Bassel, R. M. Drisko, and G. R. Stachler, Oak Ridge National Laboratory Report No. ORNL-3240 and Suppl., 1962 (unpublished).
[22] G. R. Stachler, Nucl. Phys. **55**, 1 (1964).
[23] R. N. Glover and A. D. W. Jones, Nucl. Phys. **81**, 268 (1966).

strength λ were fixed at 1.25 F, 0.65 F, and 25.0, respectively. The depth of the Woods-Saxon well V_n was then varied to reproduce the experimental neutron separation energy of the given neutron pickup transition. In those cases where the (d, t) transition corresponded to the pickup of a shell-model orbital at or below the Fermi surface the value of V_n was between 54 and 60 MeV. However, when the (d, t) transition corresponded to the pickup of a shell-model orbital above the Fermi surface the value of V_n necessary to bind this orbital at the experimental separation energy could be much greater than 60 MeV. In those cases the form factor was also calculated under the condition that r_{0n} was increased to make $V_n \cong 60$MeV. The shapes of the (d, t) DWBA angular distributions calculated with r_{0n} variable and $V_n \cong 60$ MeV were quite similar to those calculated with r_{0n} fixed at 1.25 F. However, there were considerable variations in the absolute magnitude of the DWBA cross sections, and therefore considerable variations in the deduced spectroscopic factors. It was concluded that the differences in the spectroscopic factors obtained by these two procedures would give some indication of the uncertainties in the experimental spectroscopic factors reflecting uncertainties in the assumed neutron form factor.[24]

The fits of the DWBA calculations to the experimental (d, t) angular distributions are presented in Figs. 2, 3, 4, 6, 7, 9, 10, and 11. All the DWBA curves were calculated without a radial cutoff. A radial cutoff at the nuclear surface was found to have little or no effect either on the shape or on the magnitude of the DWBA (d, t) angular distribution. With the exception of the $l_n=0$ fits for the $\frac{1}{2}^+$ 0.78-MeV Si^{27} level and for the $\frac{1}{2}^+$ 1.18-MeV Ar^{35} level, the DWBA fits for the strong (d, t) transitions studied in this experiment are reasonably good. At $E_d=21.6$ MeV, the experimental $l_n=0$ transition to the $\frac{1}{2}^+$ level in Si^{27} (Fig. 3) has a broad shoulder between 40° and 65° rather than the oscillatory behavior displayed by the experimental $l_n=0$ transitions to the $\frac{1}{2}^+$ levels in S^{31} and Ar^{35} (Figs. 6 and 10). The reason for this is not known. In some preliminary data taken at this laboratory at $E_d=21.0$ MeV the experimental $l_n=0$ transition to the 0.78 $\frac{1}{2}^+$ level in Si^{27} shows a definite minimum between 40° and 45° with a further maximum near 60°. The DWBA fit for the $l_n=0$ transition to the $\frac{1}{2}^+$ 1.18-MeV level in Ar^{35} is considerably improved if deuteron optical model parameters similar to those used in the $Si^{28}(d, t)$ DWBA calculations are also used for this $Ar^{36}(d, t)$ transition. The dotted line in Fig. 10 is the DWBA curve obtained with these parameters. The spectroscopic factors obtained from the two DWBA curves shown in Fig. 10 are almost identical.

The $l_n=2$ DWBA fit to the $\frac{3}{2}^+$ 0.96-MeV level in Si^{27} (Fig. 2) is not good. The difficulty here may lie with the experimental data. At the forward angles the errors on the experimental data are quite large; and data were obtained only for center-of-mass angles greater than 22.5°, while the DWBA curve suggests that the cross section peaks at approximately 15° to 20° in the center-of-mass system. In Fig. 2 the normalization of the DWBA curve to the experimental data is quite uncertain; this is reflected in a large uncertainty in the $l_n=2$ spectroscopic factor for this transition. DWBA analyses are not presented for the $Si^{28}(d, t)$ transitions to the $\frac{5}{2}^+$ 2.65-MeV level (Fig. 3) and to the $\frac{3}{2}^+$ 2.87–$\frac{9}{2}^+$ 2.91-MeV doublet (Fig. 4). The transition to the $\frac{5}{2}^+$ 2.65-MeV level is quite weak, and the

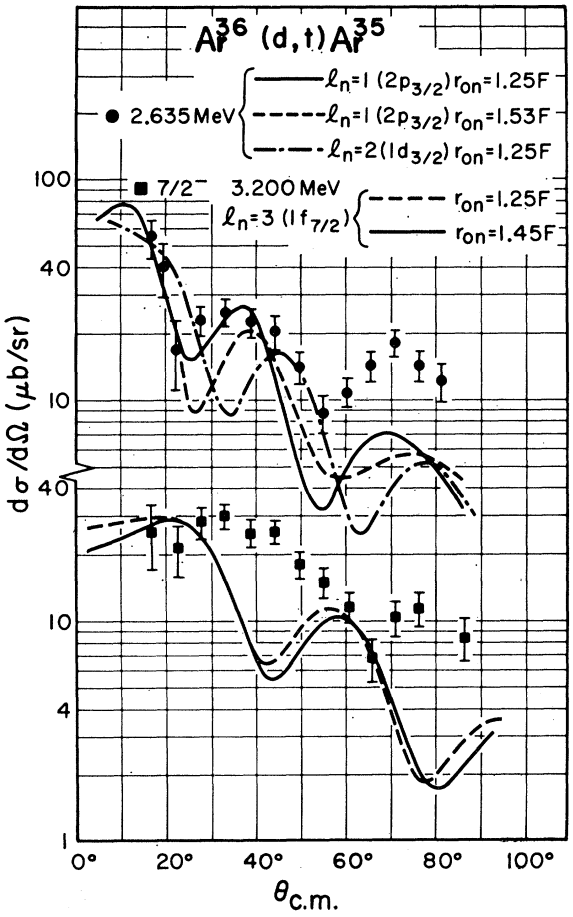

FIG. 11. Experimental $Ar^{36}(d, t)Ar^{35}$ angular distributions for the 2.635-MeV level and the $\frac{7}{2}^-$ 3.200-MeV level. The (d, t) angular distribution to the 2.635-MeV level is fitted with DWBA curves under the asumption that it represents either an $l_n=1$ $(2p_{3/2})$ transition or an $l_n=2$ $(1d_{3/2})$ transition. Two $l_n=1$ $(2p_{3/2})$ DWBA curves are presented; in one $r_{on}=1.25$ F ($V_n=78.5$ MeV), while in the other $r_{on}=1.53$ F ($V_n=60.7$ MeV). These two $l_n=1$ $(2p_{3/2})$ DWBA curves differ in absolute magnitude by a factor of 3.5. The (d, t) angular distribution to the $\frac{7}{2}^-$ 3.200-MeV level is fitted with two $l_n=3$ $(1f_{7/2})$ DWBA curves; in one $r_{on}=1.25$ F ($V_n=71.4$ MeV), while in the other $r_{on}=1.45$ F ($V_n=59.1$ MeV). The two $l_n=3$ $(1f_{7/2})$ DWBA curves differ in absolute magnitude by a factor of 3.

[24] W. T. Pinkston and G. R. Stachler, Nucl. Phys. **72**, 641 (1965).

TABLE II. Spectroscopic factors for the $Si^{28}(d, t)Si^{27}$ reaction.

Level in Si^{27}	l	This experiment $Si^{28}(d, t)Si^{27}$ $E_d=21.6$ MeV $r_{0n}=1.25$ F	This experiment r_{0n} variable $V_n\sim60$ MeV	Other neutron pickup reactions on Si^{28} (p, d) $E_p=27.6$ MeV[a]	(p, d) $E_p=33.6$ MeV[b]	(He^3, α) $E_{He^3}=10$ MeV[c]	(He^3, α) $E_{He^3}=15$ MeV[d]
G.S. $\frac{5}{2}^+$	2	4.15	4.15	2.14	3.45	2.0	2.99
0.78 MeV $\frac{1}{2}^+$	0	1.10	0.78	0.65	0.64	0.7	0.42
0.96 MeV $\frac{3}{2}^+$	2	(0.75)[e]	(0.48)[e]	0.37	0.34	0.5	0.38

[a] Reference 4.
[b] Reference 6.
[c] Reference 7.
[d] Reference 8. The spectroscopic factors in Ref. 8 are relative. In that paper the sum of the spectroscopic factors to all levels less than $E_x=3.00$ MeV was set equal to 6.00.
[e] In our experiment there is a large uncertainty in the (d, t) spectroscopic factor to the $\frac{3}{2}^+$ 0.96-MeV level in Si^{27} due to a large uncertainty in the normalization of the DWBA curve to the experimental (d, t) angular distribution.

experimental angular distribution cannot be definitely assigned as an $l_n=2$ pickup transition. The experimental angular distribution to the $\frac{3}{2}^+$ 2.87–$\frac{9}{2}^+$ 2.91-MeV doublet does not resemble an $l_n=2$ pickup transition. As was discussed in Sec. III, there is a reasonable possibility that the $\frac{9}{2}^+$ member of this doublet is rather strongly excited in the (d, t) reaction.

As shown in Fig. 11, we have attempted to fit the (d, t) angular distribution to the 2.635-MeV level in Ar^{35} assuming both $l_n=1$ $(2p_{3/2})$ neutron pickup and $l_n=2$ $(1d_{3/2})$ neutron pickup. Two $l_n=1$ DWBA curves are shown; one was calculated with the bound neutron parameter r_{0n} set equal to 1.25 F ($V_n=78.5$ MeV) while in the other r_{0n} was set equal to 1.53 F ($V_n=60.5$ MeV). In the forward angle region the experimental data are definitely fit better by the $l_n=1$ $(2p_{3/2})$ DWBA curves. An intercomparison of the experimental data by themselves shows that the forward angle structure of the 2.635-MeV $Ar^{35}(d, t)$ angular distribution is displaced some 5° to 7° toward smaller angles as compared to the strong $l_n=2$ $(1d)$ neutron pickup transitions in the $Ar^{36}(d, t)$ and $S^{32}(d, t)$ reactions. An $l_n=1$ $(2p)$ assignment for this $Ar^{36}(d, t)$ angular distribution would be in agreement with the 27.5-MeV $Ar^{36}(p, d)$ experiment of Johnson and Griffiths.[5] However, in an $Ar^{36}(p, d)$ experiment at 33.6 MeV, Kozub[6] found that the (p, d) angular distribution for the 2.635-MeV level was very similar to that for the $\frac{3}{2}^+$ Ar^{35} ground state, and he therefore assigned this transition as $l_n=2$ $(\frac{3}{2}^+)$. The present data would definitely favor an $l_n=1$ assignment for this transition, but both $l_n=1$ $(2p_{3/2})$ and $l_n=2$ $(1d_{3/2})$ spectroscopic strengths were calculated for this transition (see Table IV). If an $l_n=2$ $(1d_{3/2})$ transition is assumed, the large uncertainty in the normalization of the $l_n=2$ DWBA curve to the experimental data reflects itself in a large uncertainty in the extracted spectroscopic strength.

The experimental (d, t) angular distribution for the $\frac{7}{2}^-$ 3.200-MeV level in Ar^{35} is fitted quite poorly by $l_n=3$ $(1f_{7/2})$ DWBA curves (Fig. 11). The $l_n=3$ $(1f_{7/2})$ DWBA curves peak at approximately 20° with a minimum at 45°, while the experimental data show a broad maximum centered at 30° to 35°. The shapes of the $l_n=3$ $(1f_{7/2})$ DWBA curves are almost identical for $r_{0n}=1.25$ F ($V_n=71.4$ MeV) and $r_{0n}=1.45$ F ($V_n=59.1$ MeV), although their absolute values differ by a factor of 3. The use of a radial cutoff at the nuclear surface ($R_c=4.15$ F) does not improve the fit of the DWBA curves to the experimental data. The reason for this poor fit is not known. One possibility might be that this 3.200-MeV level in Ar^{35} is actually a doublet, but extensive studies of Cl^{35}, the mirror nucleus to Ar^{35}, have not found two levels in this energy region.[14]

V. SPECTROSCOPIC INFORMATION AND DISCUSSION

Using the relation

$$d\sigma/d\Omega_{\text{exp}}(d, t)=3.33Sd\sigma/d\Omega_{\text{DWBA}}(d, t),$$[25]

spectroscopic factors were obtained from the DWBA analyses discussed in Sec. IV. The ratios between the

TABLE III. Spectroscopic factors for the $S^{32}(d, t)S^{31}$ reaction.

Level in S^{31}	l	This experiment $S^{32}(d, t)S^{31}$ $E_d=21.0$ MeV	Other neutron pickup reactions on Si^{31} (p, d) $E_p=33.6$ MeV[a]	(He^3, α) $E_{He^3}=15.0$ MeV[b]
G.S. $\frac{1}{2}^+$	0	0.87	1.04	0.9
1.24-MeV $\frac{3}{2}^+$	2	0.55	0.98	1.1
2.23-MeV $\frac{5}{2}^+$	2	2.40	2.77	2.9

[a] Reference 6.
[b] Reference 9. The spectroscopic factors in Ref. 9 are relative. In that paper the sum of the spectroscopic factors to the $\frac{1}{2}^+$ ground state and to the $\frac{3}{2}^+$ 1.24-MeV first excited state of S^{31} was set equal to 2.00.

[25] R. H. Bassel, Phys. Rev. **149**, 791 (1966).

TABLE IV. Spectroscopic factors for the $Ar^{36}(d,t)Ar^{35}$ reaction.

Level in Ar^{35}	l	This experiment: $Ar^{36}(d,t)Ar^{35}$ $E_d=21.0$ MeV $r_{0n}=1.25$ F	This experiment: r_{0n} variable $V_n\sim60$ MeV	Other neutron pickup experiments on Ar^{36}: (p,d) $E_p=27.5$ MeV[a]	(p,d) $E_p=33.6$ MeV[b] $r_{0n}=1.15$ F	(p,d) $E_p=33.6$ MeV[b] $r_{0n}=1.35$ F
G.S. $\frac{3}{2}^+$	2	3.4	3.4	2.92	3.03	1.76
1.18 MeV $\frac{1}{2}^+$	0	1.4	1.4	2.50	1.29	1.05
1.70 MeV $(\frac{5}{2}^+)$	(2)	<0.2[c]	<0.2[c]		0.1	
2.635 MeV $(\frac{3}{2}^+)$	(2)	(0.5)[d]	(0.5)[d]		0.42[f]	0.28[f]
$(\frac{3}{2}^-)$	(1)	(0.11)	(0.032)	(0.12)[e]		
2.986 MeV $\frac{5}{2}^+$	2	2.6	2.6	2.47	2.31	1.53
3.200 MeV $\frac{7}{2}^-$	(3)	(0.33)[d]	(0.11)[d]	0.63	0.64	0.37

[a] Reference 5.
[b] Reference 6.
[c] In the present experiment the 1.70-MeV $(\frac{5}{2}^+)$ level is excited very weakly; see Sec. III. However, we are able to put an upper limit on the possible $l_n=2$ $(1d_{5/2})$ spectroscopic strength for this transition.
[d] There is a large uncertainty in the spectroscopic strength for this transition, due to a large uncertainty in the normalization of the DWBA curve with the experimental angular distribution.
[e] In Ref. 5 it was assumed that the angular distribution to the 2.635-MeV level corresponded to an $l_n=1$ $(2p_{3/2})$ neutron pickup transition.
[f] In Ref. 6 it was assumed that the angular distribution to 2.635-MeV level corresponded to an $l_n=2$ $(1d_{3/2})$ neutron pickup transition.

experimental and DWBA (d,t) angular distributions were taken from a "best fit" in which the forward angle points were weighted most heavily. Tables II–IV present the spectroscopic factors measured in this experiment for the $Si^{28}(d,t)Si^{27}$, $S^{32}(d,t)S^{31}$, and $Ar^{36}(d,t)Ar^{35}$ reactions, respectively, together with the results from other neutron pickup reaction studies on Si^{28}, S^{32}, and Ar^{36}.[4–9] In general the comparisons between the present results and those of the other neutron pickup experiments are reasonably good. In Table II the $Si^{28}(d,t)$ spectroscopic factors are shown to be systematically higher than those from the (p,d) [4,6] and (He^3,α) [7,8] experiments, but the 20% uncertainty in the experimental $Si^{28}(d,t)$ cross sections could encompass much

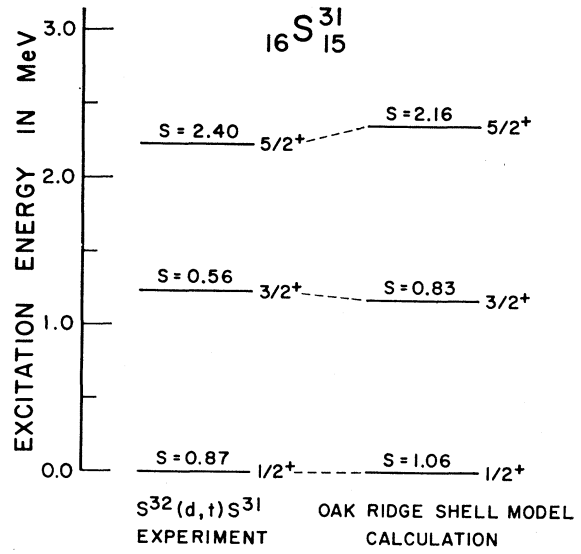

FIG. 12. Comparison of the present $S^{32}(d,t)S^{31}$ experimental results with the shell-model calculation of Ref. 27.

of this discrepancy. It should be mentioned that two experiments have been reported for the proton pickup reaction (d,He^3) on Si^{28} leading to the mirror nucleus of Si^{27}, Al^{27}.[15,26] The $Si^{28}(d,He^3)$ spectroscopic factors determined in those experiments for the first three levels of Al^{27} are in reasonable agreement with the present $Si^{28}(d,t)$ spectroscopic factors for the first three levels in Si^{27}.

An extensive set of $2s$-$1d$ shell-model calculations has been reported recently by a group at the Oak Ridge National Laboratory; this work has been summarized in a paper by Halbert.[10] In these calculations both energy level spectra and spectroscopic factors are calculated, and direct comparison can be made with the present Si^{28}, S^{32}, and $Ar^{36}(d,t)$ experimental results.

In the mass region $A=20$–28 these shell-model calculations use a truncated basis consisting of $1d_{5/2}$ and $2s_{1/2}$ particles. The two-body matrix elements in the shell-model effective interaction are determined by optimizing the fit to approximately 90 observed levels in the $20\leq A\leq28$ region. This calculation predicts that the single nucleon pickup transition from the ground state of Si^{28} to the $\frac{5}{2}^+$ ground state of either Al^{27} or Si^{27} will have a spectroscopic factor of 3.9, while the transition to the theoretically predicted $\frac{1}{2}^+$ 0.83-MeV level (experimentally there is a $\frac{1}{2}^+$ level at 0.843 MeV in Al^{27} and 0.78 MeV in Si^{27}) has a spectroscopic factor of 0.85.[10,26] These predictions are in quite good agreement with the results of our $Si^{28}(d,t)Si^{27}$ experiment (Table II). Since the shell model basis does not contain $1d_{3/2}$ particles, this presently available calculation cannot predict $l_n=2$ $(1d_{3/2})$ spectroscopic factors.

In the mass region $A=30$–33, the Oak Ridge shell-model calculations used a $1d_{5/2}$, $2s_{1/2}$, and $1d_{3/2}$ shell-

[26] B. H. Wildenthal and E. Newman, Phys. Rev. **167**, 1027 (1968).

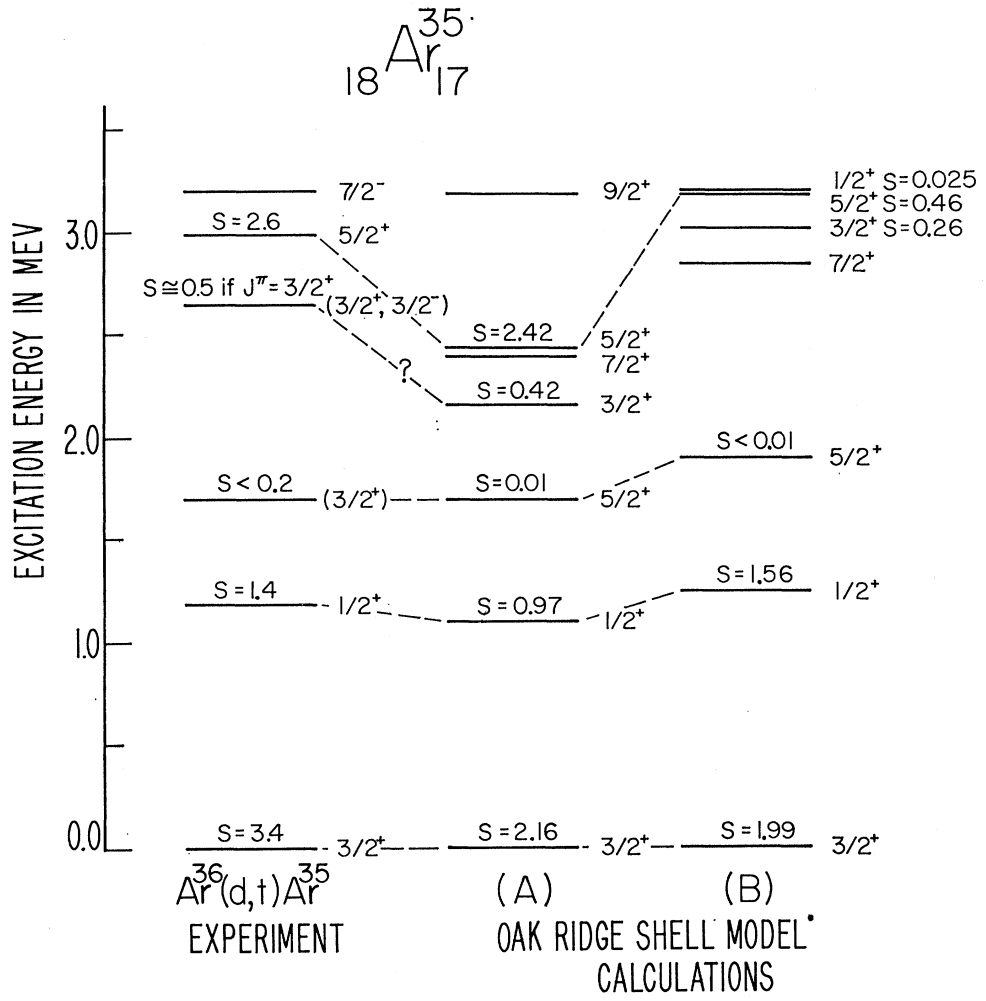

FIG. 13. Comparison of the present $Ar^{36}(d, t)Ar^{35}$ experimental results with two shell-model calculations which use a complete $2s$-$1d$ basis. Calculation (A) uses a "realistic" interaction derived from a potential which fits nucleon-nucleon scattering, while calculation (B) uses a modified surface delta interaction.

model basis, with no more than two holes being allowed in the $1d_{5/2}$ shell.[27] The effective interaction was taken to be a modified surface delta interaction (MDSI).[28] Figure 12 compares the theoretical calculation with our $S^{32}(d, t)S^{31}$ experimental results. The agreement is quite good.

In the mass region $A=34$–39, these shell-model calculations used the full space of all possible $2s$-$1d$ wave functions. Two effective interactions were used in the calculations. One was a "realistic" interaction derived from a potential which fits nucleon-nucleon scattering data,[10] while the other was the MDSI. Figure 13 compares our $Ar^{36}(d, t)Ar^{35}$ experimental results with the results of both theoretical calculations. The experimental (d, t) results agree quite well with the theoretical calculation which uses a "realistic interaction." The agreement between the (d, t) experiment and the MDSI calculation is not as good since experimentally the $l_n=2$ spectroscopic strength to the $\frac{5}{2}^+$ level in Ar^{35} at 2.985 MeV is found to be 2.6, while the MDSI calculation finds a spectroscopic strength of only 0.46 for a predicted $\frac{5}{2}^+$ level at 3.18 MeV. Also, in the MDSI calculation the next two predicted $\frac{5}{2}^+$ levels at 4.74 and 5.49 MeV have spectroscopic strengths of only 0.09 and 0.39, respectively. Thus the MDSI calculation predicts much less $l_n=2$, $1d_{5/2}$ spectroscopic strength at relatively low excitation energy in Ar^{35} than is observed experimentally.

A quite interesting comparison can be made between various theoretical predictions for the first $\frac{5}{2}^+$ levels in Ar^{35} and S^{31}. An earlier shell-model calculation of

[27] B. H. Wildenthal, J. B. McGrory, and E. C. Halbert, Phys. Letters **27B**, 611 (1968).
[28] P. W. M. Glaudemans, P. J. Brussaard, and B. H. Wildenthal, Nucl. Phys. **A102**, 593 (1967).

Glaudemans *et al.*[29] for the mass region $29 \leq A < 40$ predicted a $\frac{5}{2}^+$ level in the $T=\frac{1}{2}$ isobaric doublet Cl^{35}-Ar^{35} at 1.67 MeV, in good agreement with experiment. This theoretical calculation assumed a closed $1d_{5/2}$ shell at Si^{28}, so that the shell-model basis consisted only of $2s_{1/2}$ and $1d_{3/2}$ orbitals. Since this theoretical level $\frac{5}{2}^+$ level at 1.67 MeV has a closed $1d_{5/2}$ neutron shell, there would be no $l_n=2$, $1d_{5/2}$ spectroscopic strength to such a level in the $Ar^{36}(d, t)Ar^{35}$ reaction. Experimentally, the $l_n=2$, $1d_{5/2}$ spectroscopic strength to the first $\frac{5}{2}^+$ level in Ar^{35} at 1.70 MeV is very small, in agreement both with the calculations of Ref. 29 and the more complete shell-model calculations shown in Fig. 13. The good agreement between the $2s_{1/2}$-$1d_{3/2}$ shell-model calculation of Ref. 29 and experiment for the first $\frac{5}{2}^+$ level in Ar^{35} can be contrasted with the rather poor agreement between this calculation and experiment for the first $\frac{5}{2}^+$ level in S^{31}. In S^{31} the first $\frac{5}{2}^+$ level is found experimentally at 2.23 MeV, while the calculation of Ref. 29 predicts the first $\frac{5}{2}^+$ level at 3.18 MeV. This rather poor agreement is not surprising since both experiment and the more complete shell-model calculations of Ref. 27 agree that there is a large $1d_{5/2}$ neutron hole component in the wave function for this level (Fig. 12); the shell-model basis of Ref. 29 does not include $1d_{5/2}$ neutron holes.

The Si^{28}, S^{32}, and $Ar^{36}(d, d')$ scattering studies at this laboratory[1] have indicated that Si^{28} most probably has an oblate static deformation while S^{32} and A^{36} appear to be spherical vibrational nuclei. At least for S^{32} and Ar^{36}, the good agreement between the spherical model calculations[10] and the present $S^{32}(d, t)$ and $Ar^{36}(d, t)$ experimental results would tend to reinforce the conclusion drawn from the (d, d') work that the equilibrium shape of nuclei in the upper half of the *s-d* shell changes from a poorly stabilized oblate shape at $A=28$ to a spherical equilibrium shape at $A=32$, with this spherical equilibrium shape being retained up to the end of the shell at $A=40$. However, it should be emphasized that the extent to which agreement between the spherical shell-model calculations and experiment can be used to indicate that the nuclei under consideration indeed have spherical equilibrium shapes is very much open to question. For example, it is well established that Ne^{21} is a strongly deformed nucleus[30,31]; at the same time the spherical shell-model calculations[10] are successful in fitting the energy level sequence of the $K=\frac{3}{2}$ ground-state band for this nucleus quite well.

Any simple rotational model is certainly at variance with our experimental results. For single nucleon pickup transitions in this model, there is a sum rule limit of two on the spectroscopic factors to levels where K is a good quantum number—no band mixing. Experimentally, this limit is certainly violated in the $l_n=2$, $1d_{5/2}$ $Si^{28}(d, t)Si^{27}$ ground-state transition, and is probably violated by one $S^{32}(d, t)S^{31}$ transition and two $Ar^{36}(d, t)Ar^{35}$ transitions (see Tables III and IV).

The weak-coupling model[32,33] presents a rather simple framework in which the low-lying energy structure of odd-even nuclei can be discussed. In this model a single particle or hole couples both to the 0^+ ground state of an adjacent even-even nucleus and to a collective excitation (usually 2^+) of this same nucleus, producing the low-lying energy structure of the odd-even nucleus. In the case of Al^{27}, where a $1d_{5/2}$ proton hole is coupled to the ground state and first excited 2^+ level in Si^{28}, the weak-coupling model is able to explain rather well both the level structure of Al^{27} up to 3 MeV [34] and the relative excitation of these levels in inelastic scattering.[35] Al^{27} is the mirror nucleus to Si^{27}, whose structure was studied in the present $Si^{28}(d, t)$ experiment. Inelastic proton scattering on P^{31}, the mirror nucleus to S^{31}, indicated that the weak-coupling model may also have some validity for this nucleus.[35] It would be very interesting to perform an inelastic scattering experiment on Cl^{35}, the mirror nucleus to Ar^{35}, in order to determine whether its low-lying energy level structure could also be discussed within the framework of the weak-coupling model.

In conclusion, we find that the current ORNL shell-model calculations provide rather excellent reproduction of the available data pertaining to the Si^{27}, S^{31}, and Ar^{35} systems; this is most gratifying in light of the relative complexity of these calculations. At the same time the present data do not provide significant insight into the question of the equilibrium shape of nuclei in the upper end of the *sd* shell beyond that already reported from our deuteron scattering studies.

ACKNOWLEDGMENTS

We would like to thank Kenzo Sato and the operating staff of the A. W. Wright Nuclear Structure Laboratory for their assistance during the running of these experiments. Dr. A. Howard and Dr. W. W. Watson of the Yale Isotope Separation Group provided us with the Ar^{36} used in this work; and Dr. Howard assisted us during the $Ar^{36}(d, t)$ runs. We would also like to thank the Oak Ridge Theoretical Group of Dr. E. Halbert, Dr. P. W. M. Glaudemans, Dr. J. B. McGrory, and Dr. B. H. Wildenthal for providing us their recent $2s$-$1d$ shell-model calculations.

[29] P. W. M. Glaudemans, G. Wiechers, and P. J. Brussaard, Nucl. Phys. **56,** 548 (1964).
[30] A. J. Howard, J. P. Allen, and D. A. Bromley, Phys. Rev. **139,** B1135 (1965).
[31] A. J. Howard, J. P. Allen, D. A. Bromley, J. W. Olness, and E. K. Warburton, Phys. Rev. **157,** 1022 (1967).
[32] R. D. Lawson and J. L. Uretsky, Phys. Rev. **108,** 1300 (1957).
[33] A. de-Shalit, Phys. Rev. **122,** 1530 (1960).
[34] V. K. Thankappan, Phys. Rev. **141,** 957 (1966).
[35] G. M. Crawley and G. T. Garvey, Phys. Rev. **167,** 1070 (1968).